Heliyon 10 (2024) e24734

Contents lists available at ScienceDirect

Heliyon

journal homepage: www.cell.com/heliyon

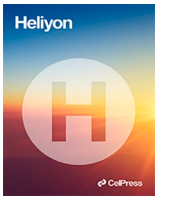

Research article

Experimental surface runoff hydrographs from linear impervious subcatchments for rainfalls of extremely high intensity

Volodymyr Zhuk, Lesya Vovk *, Ihor Popadiuk, Ivan Matlai

Lviv Polytechnic National University, Institute of Civil Engineering and Building Systems, S. Bandera Str. 12, Lviv, 79013, Ukraine

ARTICLE INFO

Keywords:
High intensity rainfall
Linear subcatchment
Nonlinear reservoir method
Stormwater hydrograph
Surface runoff
Wave effect

ABSTRACT

This study focuses on lab-scale experimental runoff hydrographs from a linear completely impervious plane subcatchment. An improved method of surface runoff physical modelling was developed, allowing for expanded laboratory hydrograph simulations up to a linear scale of 10. Model rains of different intensities and durations were applied, and digital online data processing techniques were employed to ensure high time resolution and accurate flow rate determination. The experimental hydrographs were analyzed in a dimensionless form to facilitate generalization and comparison with widely used nonlinear reservoir method and unit hydrograph method. Wave-like fluctuations of the flow rate were observed in most experimental hydrographs as they approached the maximum runoff. The dimensionless phase time of the experimental hydrographs showed an increasing trend with higher rainfall intensity, and a power-law equation was derived to approximate this relationship. An averaged dimensionless runoff hydrograph was obtained by processing individual hydrographs, and it was approximated by the DR-Hill-Zerobackground model for the initial stage during the rainfall and by the Weibull model for the later stage, after the rainfall stopped. The findings of this study have significant implications for modelling surface runoff from small urban subcatchments, particularly under critical rainfall events with extremely high intensity.

1. Introduction

The initial stage of stormwater modelling for urbanized catchments involves establishing relationships between rainfall parameters and surface runoff hydrographs for each specific subcatchment [1–4]. Surface runoff hydrographs from subcatchments serve as crucial input functions that form the runoff hydrographs for urban catchments of varying scales, configurations, and complexities [5–9]. Methods for modelling surface runoff should comprehensively consider a multitude of factors and specific characteristics of the subcatchment, including its configuration [10–13], absolute dimensions [14,15], slope distribution at the subcatchment's area [16,17], surface cover types and their spatial distribution [18,19], correlation between the total and effective imperviousness [2,4,20,21], infiltration properties of soils [11,22–24] etc. Errors at this initial stage of modelling inevitably and often significantly impact the subsequent modelling of the entire stormwater drainage system [25,26].

Among the large number of rainfall−runoff models, hydraulically based methods, such as the kinematic wave and dynamic wave methods in various modifications [3,5,14,27,28] and the nonlinear reservoir method [11,29] should be considered the most theoretically justified. The nonlinear reservoir method, despite a significant number of simplifications, is widely used in specialized

* Corresponding author.
E-mail address: lesia.i.vovk@lpnu.ua (L. Vovk).

https://doi.org/10.1016/j.heliyon.2024.e24734
Received 13 November 2023; Received in revised form 12 January 2024; Accepted 12 January 2024
Available online 14 January 2024

application programs, such as SWMM [3,5,30,31].

The simplicity of the implementation of the nonlinear reservoir method compensates for the number of fairly obvious disadvantages, including a very schematic, approximate consideration of the subcatchment configuration by representation of the real subcatchment using a rectangular one of the same area with an effective width B_{ef}, as well as a uniform increasing of the retention layer over the entire subcatchment and the lack of consideration the effects of surface flow concentration in the direction to the stormwater inlet [5,27].

The specific multifactor physics and relatively large scales of stormwater runoff from urban areas complicate the experimental verification of rainfall−runoff models [5,32]. The performance of field experiments on real urban subcatchments is associated both with the problems of reproducing the necessary fixed initial and boundary conditions of the experiment, as well as with special requirements for technical means of monitoring and problems with the accuracy of measuring flow parameters [2,33–35]. In laboratory modelling of surface runoff, it is much easier to ensure repeatability of surface runoff over time [30,36]. At the same time, in laboratory modelling, there is a difficult to correctly solve a problem of scaling sufficiently extensive natural phenomena in the scale of laboratory installation [37–40]. Therefore, in most of the previous laboratory studies of stormwater runoff hydrographs, the dimensions of subcatchments were used as large as possible in laboratory conditions, for example, 12.19 × 12.19 m in Ref. [14], 13.4 × 2.5 m in Ref. [17], 5 × 1.25 m in Ref. [40], 1.5 × 1.5 m [41]. A linear scale of $C_L = 1$ was declared, although, in fact, dimensions of the indicated subcatchments are still significantly less comparing the typical natural subcatchments and they can be considered as non-scaled only with some approximation. At the same time, a very small number of experimental laboratory studies concerned rains of particularly high intensity, for example, 60–300 mm/h in Ref. [14], 90–150 mm/h in Ref. [17], 30–90 mm/h in Ref. [16] whereas rainfalls of this order of intensities are critical in modelling surface runoff from typical small urban subcatchments.

In order to increase the reliability and accuracy of hydrological-hydraulic models of stormwater runoff from urbanized subcatchments, improving of hydraulically based methods of surface runoff modelling, is still relevant. The maximum possible number of input factors, as well as systematic experimental verification of these models should be used. Special gaps are solving the scaling problem for modelling urbanized subcatchments in laboratory conditions, and obtaining experimental runoff hydrographs for rainfalls of extremely high intensity.

The purpose of the article is to obtain experimental runoff hydrographs from linear completely impervious plane surfaces for especially high-intensity rainfall events, generalization and comparative analysis of the obtained results with hydrographs according to other most common models. The objectives of the study are obtaining the generalized experimental stormwater runoff hydrographs from linear impervious subcatchments with constant longitudinal slope in the range of 0.01–0.02 for model rainfalls of especially high intensities, and comparing these results with theoretically ones predicted by the nonlinear reservoir method and kinematic wave unit hydrograph (KWUH).

2. Materials and methods

2.1. Scale factors of the model surface runoff

An improved approach to physical modelling of surface runoff has been developed to expand the range of laboratory simulations. This method involves the integration of scale factors for key surface runoff parameters. At the linear scale of the subcatchment, within the C_L range of 5–10, it is assumed that the scale of flow depth h in all relevant cross-sections of both the prototype and the model is consistent, denoted as $C_h = 1$. When modelling surface runoff based on the Froude number [42]:

$$\mathrm{Fr} = V\,(\mathrm{gh})^{-1/2} \tag{1}$$

condition Fr − idem requires that the scale of average velocity should be $C_V = 1$.

Considering that hydraulic radius of shallow surface flows is approximately equal to the flow depth ($R \approx h$), the Shezy-Manning equation [13]:

$$V = h^{2/3}\,S^{1/2}\,n^{-1} \tag{2}$$

When the prototype and model subcatchments are geometrically similar, their respective longitudinal slopes S are the same, and the scale of the slope C_S is equal to 1. Consequently, as it follows from Eq. (2), the scale of the surface Manning's roughness coefficient C_n is also equal to 1. This equivalence is particularly advantageous for the technical implementation of hydraulic modelling.

Based on the principle of flow continuity, when scaling the flow width at $C_b = C_L$, the scale of surface runoff discharge C_Q is also C_L. To ensure the accuracy of hydraulic modelling, it is crucial that the scales of various flow rates were the same at corresponding time points. This alignment results in a scale for rainfall discharge $C_{Q.r}$ equal to C_L, leading to a scale for rainfall intensity $C_{i.r} = C_L^{-1}$. In this proposed scaling scheme, the time scale is $C_t = C_L/C_V = C_L$, while the volumes of rain and surface runoff for both the prototype and the model are scaled as $C_W = C_{Q.r}\,C_t = C_L^2$.

Another advantage of this scaling scheme is the correspondence of surface flows in both the prototype and model, particularly in terms of the Reynolds number [42]:

$$\mathrm{Re} = V\,h\,\nu^{-1} \tag{3}$$

where ν is kinematic viscosity, as well as the Weber number [42]:

$$\mathrm{We} = \rho V^2 h \sigma^{-1} \tag{4}$$

where σ is the surface tension. Achieving the conditions of Re – idem and We – idem is particularly important for the accurate physical modelling of shallow surface flows. This eliminates risks about potential discrepancies in Reynolds numbers and, consequently, flow modes between the prototype and the model. It also resolves the issue of distortion in the physical representation of flow on the model due to non-scaled surface tension forces.

Considering that the surface runoff is characterized by a predominantly unsteady flow mode, it is important to obtain the similarity by the Strouhal number [42]:

$$\mathrm{St} = L\, V^{-1} t^{-1} \tag{5}$$

The proposed scaling scheme assumes that $C_V = 1$ and $C_t = C_L$, resulting in St – idem.

The significant advantage of the provided set of scaling factors is the uniform scaling of all terms in the Saint-Venant differential equation, expressed in the kinematic wave equation form, all of which are equivalent to C_L^{-1}.

2.2. Surface runoff experimental set-up

For the experimental study of stormwater hydrographs, the laboratory setup was designed (Fig. 1). It consisted of a rainfall simulator, an inclined impervious plane hydraulic flume, and an online system for recording the surface hydrographs [41].

A specialized rainfall simulator was utilized to generate precipitation at various intensities, reaching up to 40 mm/min. Water supply to the experimental setup was maintained by employing a large source tank with a 3.0-m diameter, featuring a free water surface positioned approximately 22 m above the axis of the distribution pipeline (1). The flow rate at the inlet of the experimental setup was measured using a water meter (6) Gross MNK-UA 25/260, with a relative measurement error of ±2.0 %. The pressure distribution pipeline (1), spanning a length of 6.0 m, was connected to the source tank and equipped with a bypass pipeline (2), enhancing the even distribution of rainfall intensity along the distribution pipeline's length. The distribution pipeline (1) had perforations with a 2 mm diameter and a constant spacing of 5 cm. Regulation of the water flow rate through the distribution pipeline (1) was achieved using valve (3). To maintain a consistent rainfall intensity, an intercepting tray (4) was placed beneath the distribution pipeline. Upon opening valve (3), this tray redirected water away from the hydraulic flume until the flow rate equalized along the entire length of the distribution pipeline (1). Subsequently, the tray was repositioned, and the experiment commenced.

The water from pipeline (1) flowed into the hydraulic flume (5) with the following dimensions: length $L = 6.0$ m, width $b = 0.305$ m, and height 0.4 m (Fig. 1). The laboratory setup was equipped with a slope-adjusting system that allowed the study of surface runoff hydrographs at different longitudinal slopes of the flume. The mean measured value of the Manning's roughness coefficient for the hydraulic flume was determined to be $n = 0.009 \pm 0.0003$, and the longitudinal slope of the flume ranged from $S = 0.01$ to 0.02, with accuracies in the range of ±(1.0–0.5)%, respectively.

The surface runoff freely entered the detention tank (7), which had a volume of 45 L. The real-time data of the current mass of the surface runoff were measured by the digital scale AXIS BDU-60 (8), and transmitted each 0.125 s to the computer using the RS-232 module. Absolute error of mass measurement was equal to ±10 g. The runoff volume at any given moment t was determined as a

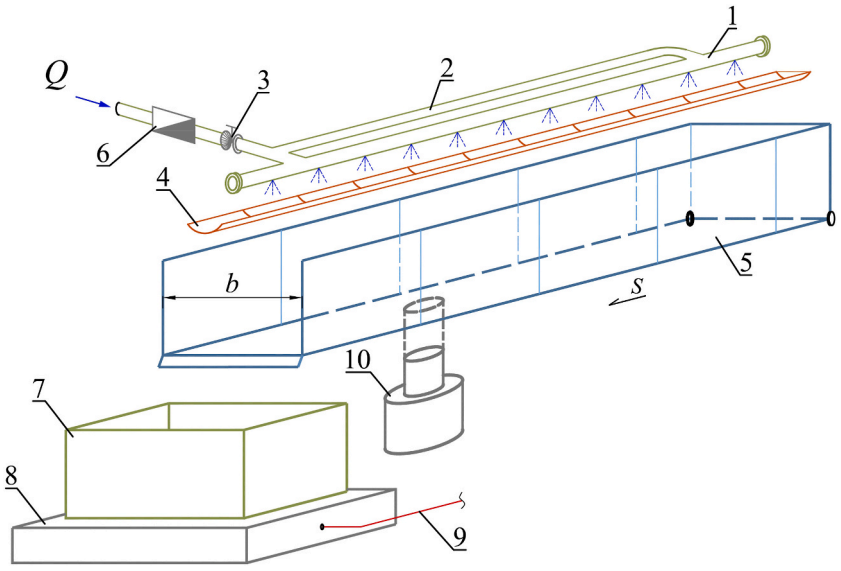

Fig. 1. Surface runoff experimental set-up: 1 – water distribution pipeline; 2 – bypass pipeline; 3 – valve; 4 – interception tray; 5 – hydraulic flume; 6 – water meter; 7 – detention tank; 8 – digital scale AXIS BDU-60; 9 – digital output to the computer; 10 – slope adjuster.

fraction of the inflow mass and the specific mass of tap water, which varied depending on water temperature in the range of 19–25.6 °C. To assess the reproducibility of runoff hydrographs, four repetitions were conducted for each rainfall intensity.

2.3. Processing of experimental results

In this series of studies, runoff hydrographs were simulated for rainfalls of constant intensity and duration from 35 s to 50 s. By definition, the intensity of model rain:

$$i_r = W_r \ / \ (A \times t_r) \tag{6}$$

W_r, t_r – total volume and duration of model rain, respectively; A – the area of the model subcatchment, $A = 1.83$ m^2.

Intensities of model rainfalls varied in the range of 473–2176 mm/h, which corresponds to prototype intensities 47.3–217.6 mm/h, for maximum linear scale $C_L = 10$ of the presented laboratory model. The duration of model rainfalls ranging from 35 to 50 s at scale $C_t = C_L = 10$ corresponds to prototype rainfall durations of 350–500 s. This range covers the surface runoff concentration time for small subcatchments with a concentration length of up to 60 m.

The volume flow of surface runoff was calculated through numerical differentiation of the function $W(t)$, which was provided in tabular form. The volume curve around the point ($t_0 \pm \Delta t/2$) was approximated using a quadratic trend line:

$$W(t) = a_1 t^2 + a_2 t + a_3 \tag{7}$$

where t_0 is the current central time point; Δt – the time interval within which volume values were taken for processing; a_1, a_2, a_3 – empirical regression coefficients depending on t_0, found using the least square method.

By differentiating Eq. (7), the flow rate of the surface runoff at time t_0:

$$Q(t_0) = 2a_1 t_0 + a_2 \tag{8}$$

The issue of selecting the optimal time interval, Δt, was examined separately. Increasing this interval stabilizes the $Q(t)$ function, eliminating local jumps, but it also results in excessive inertial smoothing of runoff hydrographs, particularly in transition sections. Comparative analysis revealed that with a specified data update frequency of 0.125 s, the optimal time interval was determined to be $\Delta t = 2.5$ s.

Relative errors of the experimental determination of main parameters were as follows: 0.5–1.0 % for longitudinal slope, 2.9–3.2 % for rainfall intensity, and 2.6–2.9 % for maximum runoff discharge.

3. Results and discussion

3.1. Experimental surface runoff hydrographs

An example of the primary results of an experimental study of model surface runoff from one model rainfall event is shown in Fig. 2. Runoff volume $W(t)$ was directly measured with digital scale AXIS BDU-60. Rain volume was defined as the product of rainfall intensity and current time at $t \le t_r$, and after rain stops, at $t > t_r$, it was constant and equal to the total rainfall volume W_r. The volume retained on the surface at any moment of time was determined as the difference between the corresponding rainfall volume and the volume of runoff. The area-averaged depth of the surface retention layer was calculated in order to further compare the experimental results with numerical modelling using the nonlinear reservoir method.

Dimensional model runoff hydrographs, obtained by the method of numerical differentiation of experimental runoff volume $W(t)$, described in subsection 2.3, for longitudinal slopes $S = 0.01$, 0.015, 0.02 are presented in Figs. 3–5 respectively.

All experimental runoff hydrographs from completely impervious plane linear subcatchments are characterized by the presence of a well-defined section of initial retention, at which the surface runoff is either absent at all, or is within the limits of the sensitivity of the digital scale, namely about 0.03 L. The rising limbs of the experimental hydrographs at $t \le t_r$ are S-shaped curves with a sharp

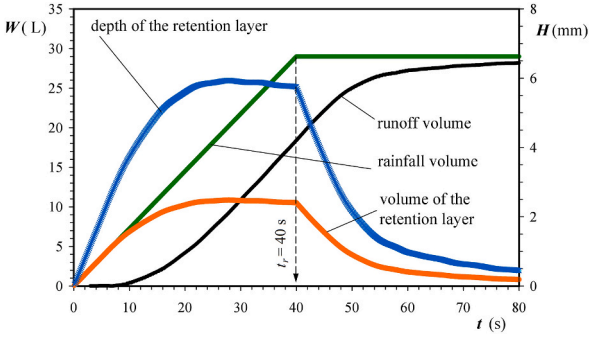

Fig. 2. Experimental curves of volumes and depths of the model runoff for $L = 6$ m; $b = 0.305$ m, $S = 0.01$; $n = 0.009$, $i_r = 1426$ mm/h; $t_r = 40$ s.

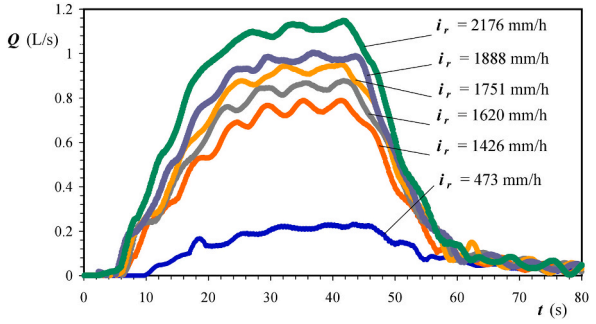

Fig. 3. Experimental hydrographs of surface runoff on the physical model: $L = 6$ m, $b = 0.305$ m, $n = 0.009$, S = 0.01.

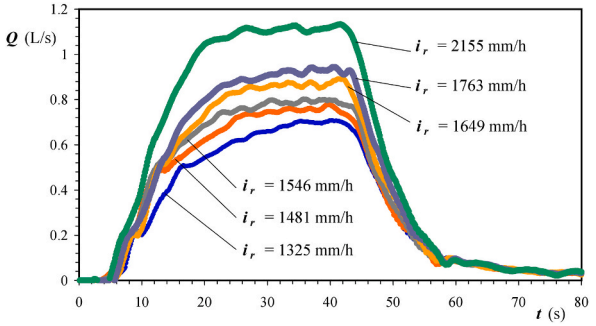

Fig. 4. Experimental hydrographs of surface runoff on the physical model: $L = 6$ m, $b = 0.305$ m, $n = 0.009$, S = 0.015.

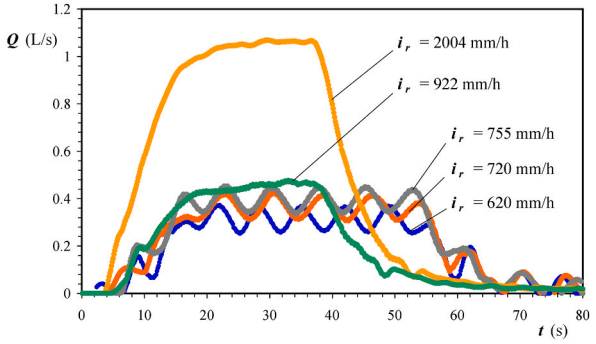

Fig. 5. Experimental hydrographs of surface runoff on the physical model: $L = 6$ m, $b = 0.305$ m, $n = 0.009$, $S = 0.02$.

increase in discharge in the first half, inflection points and an asymptotic approach to the maximum flow rate in the second half. Taking into account the completely impervious cover of the model subcatchment, the maximum runoff flow, within the error of the experimental determination, was equal to the flow rate of the model rain $Q_r = A \cdot i_r$.

Thus, the ascending limbs of hydrographs are qualitatively well correlated with similar results obtained using the nonlinear reservoir method [29]. The quantitative assessment of the asymptotic output of the flow rate to the maximum value of Q_r is complicated by the presence of the wave-like nature of the surface runoff, which becomes more pronounced with a decrease in the increment of the hydrograph to the time axis.

Such a wave nature of surface runoff depends on many partial factors and is quite common, when the flow rate is determined sufficiently accurately and with a high update frequency [14,16,40]. Waveless hydrographs in previous studies were obtained as usual at longer time steps, when instantaneous flow rates are averaged and, accordingly, hydrographs are too smoothed [13,29].

The descending limbs of experimental hydrographs at $t > t_r$ are represented by hyperbolic-type curves with a sharp decrease in flow within 15–20 s after the cessation of model rain, followed by a smooth asymptotic decrease of discharge to zero. The change in the inflow volume in different series, depending on the rainfall intensity and the longitudinal slope, reached the limit of sensitivity of the digital scale 5–7 min after the start of the model rain. To enhance the accuracy of volume determination for surface runoff, the recording duration for all series was set to 10 min, allowing for a slight reserve. The descending limbs of the model hydrographs at $t > t_r$

are similar to the corresponding curves obtained by the nonlinear reservoir method, but are characterized by a faster decrease in surface runoff compared to the last one. When flow rate is approaching to zero, regular wave phenomena are also recorded, but with smaller amplitude of the flow fluctuation and with a shorter phase duration, compared to the wave processes on the crest of the hydrograph (Figs. 3–5).

3.2. Wave parameters of experimental surface hydrographs

Wave effects observed in the majority of experimental hydrographs were subjected to statistical analysis. The primary parameters characterizing wave phenomena included the average phase time and the flow rate amplitude of the hydrographs. The reliability of the results was assessed through tests for homogeneity and normality. The findings from rainfall events of different intensities were consolidated and presented in the form of dimensionless phase times ($\Delta t_{ph}/t_r$) and dimensionless wave amplitudes ($\Delta Q_{ph}/Q_r$). Due to the limited data available on phase time and wave amplitude, a statistical analysis was conducted using Fisher's Least Significant Difference test to evaluate the significance of the results.

Dimensionless wave amplitudes of experimental hydrographs increase with decreasing the rainfall intensity, as well as with an increase in longitudinal slope (Fig. 6). The obtained results qualitatively align well with the findings of previous research. For instance, for model rainfalls with an intensity of 30 mm/h, an increase in the slope of the subcatchment from $S = 0.02$ to $S = 0.03$ led to an increase in the dimensionless wave amplitude $\Delta Q_{ph}/Q_r$ from 6.8 % to 10 % [16].

Ben-Zvi [14] reported decreasing of the dimensionless wave amplitudes for runoff hydrographs with increasing the rainfall intensity. Specifically, for a longitudinal slope of $S = 0.03$ and a steady rainfall intensity of 54 mm/h, the value of $\Delta Q_{ph}/Q_r$ about 22 % was obtained, while at intensity of 287 mm/h, it was only 17 %. De Lima et al. [40], for a longitudinal slope of $S = 0.05$ and rainfall intensities ranging from 56 to 593 mm/h, obtained a slightly lower relative wave amplitude of 7.7 % of Q_r. This difference can be attributed to the movement of the rainfall front upstream the flow at a velocity of 0.07 m/s.

Dimensionless phase time of experimental hydrographs increases with increasing the rainfall intensity (Fig. 7), moreover, for both slopes, the results are within the margin of error and can be approximated quite well by a power-law trend line:

$$\Delta t_{ph} / t_r = 0.003\ i_r^{0.444} \tag{9}$$

3.3. Dimensionless surface runoff hydrographs

Experimental hydrographs were reduced to a generalized form, as the dependences of the dimensionless flow rate Q/Q_r on the dimensionless time t/t_r (Fig. 8). The rising limbs of dimensionless experimental hydrographs are significantly steeper compared to the corresponding section of the hydrograph, obtained by the nonlinear reservoir method, which can be explained by the overestimated inertia of the last one, since, by definition, in nonlinear reservoir model, the depth of the retention layer increases equally over the entire area of the subcatchment, and the flow of surface runoff is a function of this depth.

Obtained experimental results confirm the inefficiency and inapplicability of the UHM for modelling the surface runoff from small urbanized subcatchments. The UHM was developed and still widely used for large river catchments [43–45]. The universal dimensionless hydrograph of runoff according to UHM is characterized by a slower increase in surface runoff at the first stage, when $t/t_r \leq 1$, as well as a smooth decrease in runoff over a very long period of time after the rain stops. Such a difference is explained by the apparently fundamental difference in both the runoff areas and the runoff coefficients of the urbanized and natural runoff catchments. For completely impervious subcatchments, under conditions of rainfall events of maximum intensity, this difference becomes extremely large. The occurrence of a slight excess in the dimensionless discharge $Q/Q_r = 1$ was also observed in previous studies [16]. This temporary excess can be attributed to the first flush of the surface runoff accumulated on the subcatchment, as well as the wave characteristics of the hydrographs. However, to quantitatively assess this first-flush effect, a considerably larger number of

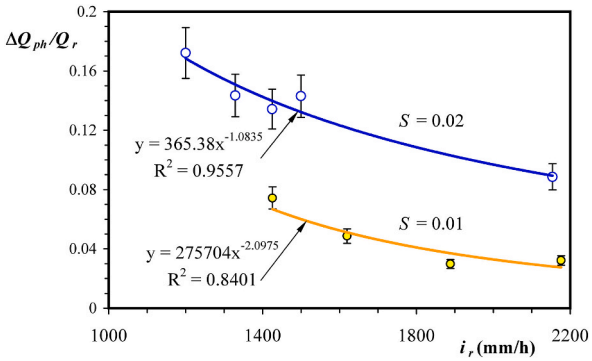

Fig. 6. Dimensionless wave amplitudes of experimental hydrographs; error bars ±10 % are specified.

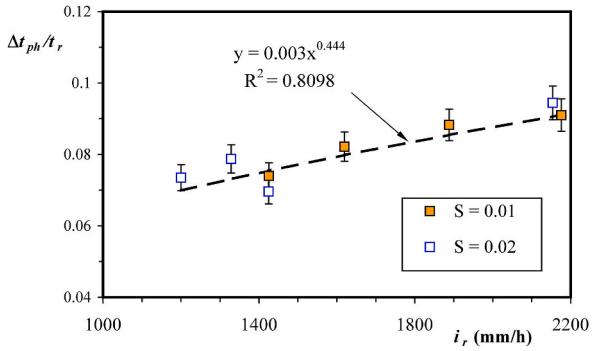

Fig. 7. Dimensionless phase time of waves on experimental hydrographs; error bars ±5 % are specified.

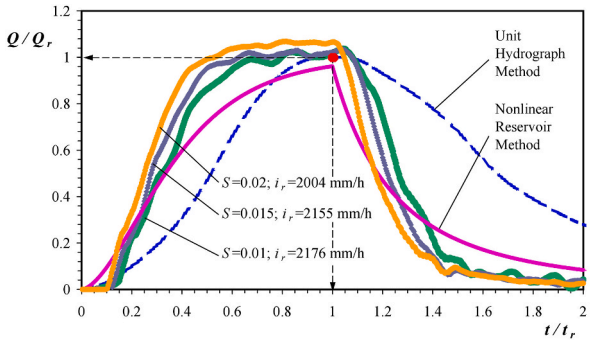

Fig. 8. Experimental dimensionless hydrographs from linear impervious plane subcatchment for model rainfalls of extremely high intensity comparing to other most common methods.

experimental hydrographs should be analyzed, especially for rainfall events of longer duration.

An averaged dimensionless runoff hydrograph from impervious plane linear subcatchment was obtained by processing dimensionless experimental runoff hydrographs. This universal hydrograph is well approximated by the DR-Hill-Zerobackground nonlinear regression model ($R^2 = 0.9987$). At the first stage, when $t/t_r \leq 1$:

$$Q / Q_r = 1.014\ (t / t_r)^{3.4} / [(t / t_r)^{3.4} + 0.014] \tag{10}$$

The second stage of the dimensionless hydrograph $t/t_r > 1$ is best approximated by the Weibull model ($R^2 = 0.9991$):

$$Q / Q_r = 1 - exp\ [-5.2\ (t / t_r)^{-10.5}] \tag{11}$$

In the future, conducting similar experimental studies for rainfall events with extremely high intensities from urbanized subcatchments holds promise. This includes studying hydrographs from subcatchments with significantly large longitudinal slopes as well as those with near-zero slopes. Additionally, it is important to conduct a detailed and systematic study of the quantitative parameters of wave phenomena in runoff hydrographs at each characteristic stage. This will involve obtaining extended samples to ensure statistically significant results.

4. Conclusions

Lab-scale experimental runoff hydrographs from a linear completely impervious plane subcatchment with length of 6.0 m, width of 0.305 m, and a cover with Manning roughness coefficient of 0.009 are obtained for especially high-intensity rainfall events at longitudinal slopes of subcatchment ranging from 0.01 to 0.02.

An improved method of surface runoff physical modelling was developed which permit expanding the range of laboratory hydrograph simulations up to the linear scale $C_L = 10$. Intensities of model rains varied in the range of 473–2176 mm/h, which corresponds to prototype intensities 47.3–217.6 mm/h. The duration of model rainfalls ranging from 35 to 50 s corresponding the prototype rainfall durations of 350–500 s. Digital online data processing with time step of 0.125 s and improved method of numerical differentiation of volume – time function were applied, which made it possible to ensure high time resolution of hydrographs and increased accuracy of flow rate determination.

Experimental hydrographs were represented in the dimensionless form to make it possible generalization of experimental results and comparison with modelling by widely used nonlinear reservoir method and UHM. The rising limbs of dimensionless experimental

hydrographs are significantly steeper compared to the corresponding section of the hydrograph, obtained by the nonlinear reservoir method and by the UHM, which can be explained by the overestimated inertia of the last ones. At asymptotic approach to the maximum runoff wave-like fluctuations of the flow rate are obtained in the majority of experimental hydrographs. Dimensionless phase time of experimental hydrographs increases with increasing the rainfall intensity, and for slopes in range 0.01–0.02 it can be approximated by a single power-law Eq. (9). An averaged experimental dimensionless runoff hydrograph from impervious plane linear subcatchment was obtained by processing the individual hydrographs. The first stage of averaged hydrograph ($t/t_r \leq 1$) is approximated by the DR-Hill-Zerobackground model (Eq. (10)), and the second stage, at $t/t_r > 1$, by Weibull model (Eq. (11)).

The obtained experimental results have particular relevance for the modelling of surface runoff from small urban subcatchments under the condition of critical rainfall events of particularly high intensity. The recommended limitation on the maximal length of the runoff subcatchments to be about 60 m. This range is suitable for the most urbanized impervious surfaces, typical for highways, parking lots, pedestrian locations, etc.

Data availability statement

Data will be made available on request.

Additional information

No additional information is available for this paper.

CRediT authorship contribution statement

Volodymyr Zhuk: Writing - original draft, Supervision, Methodology, Conceptualization. **Lesya Vovk:** Writing - review & editing, Software, Data curation. **Ihor Popadiuk:** Methodology, Investigation, Formal analysis. **Ivan Matlai:** Visualization, Validation, Software, Investigation.

Declaration of competing interest

The authors declare that they have no known competing financial interests or personal relationships that could have appeared to influence the work reported in this paper.

Acknowledgement

This research was supported by the Ministry of Education and Science of Ukraine, grant number M/56-2022 “Ecological and economic stormwater management in urban areas addressing first-flush phenomena".

References

[1] A.E. Barbosa, J.N. Fernandes, L.M. David, Key issues for sustainable urban stormwater management, Water Res. 46 (20) (2012) 6787–6798, https://doi.org/10.1016/j.watres.2012.05.029.
[2] J. Chen, B.J. Adams, Development of analytical models for estimation of urban stormwater runoff, J. Hydrol. 336 (3–4) (2007) 458–469, https://doi.org/10.1016/j.jhydrol.2007.01.023.
[3] T.D. Fletcher, H. Andrieu, P. Hamel, Understanding, management and modelling of urban hydrology and its consequences for receiving waters: a state of the art, Adv. Water Resour. 51 (2013) 261–279, https://doi.org/10.1016/j.advwatres.2012.09.001.
[4] L.A. Juma, N.V. Nkongolo, J.M. Raude, C. Kiai, Assessment of hydrological water balance in Lower Nzoia Sub-catchment using SWAT-model: towards improved water governace in Kenya, Heliyon 8 (7) (2022), https://doi.org/10.1016/j.heliyon.2022.e09799.
[5] J. Gironás, J.D. Niemann, L.A. Roesner, F. Rodriguez, H. Andrieu, A morpho-climatic instantaneous unit hydrograph model for urban catchments based on the kinematic wave approximation, J. Hydrol. 377 (3–4) (2009) 317–334, https://doi.org/10.1016/j.jhydrol.2009.08.030.
[6] Y. Seo, A.R. Schmidt, M. Sivapalan, Effect of storm movement on flood peaks: analysis framework based on characteristic timescales, Water Resour. Res. 48 (5) (2012) W05532, https://doi.org/10.1029/2011WR011761.
[7] B. Szeląg, G. Łagód, A. Musz-Pomorska, M.K. Widomski, D. Stránský, M. Sokáč, R. Babko, Development of rainfall-runoff models for sustainable stormwater management in urbanized catchments, Water 14 (13) (2022) 1997, https://doi.org/10.3390/w14131997.
[8] A. Szpak, J. Modrzyńska, J. Piechowiak, Resilience of Polish cities and their rainwater management policies, Urban Clim. 44 (2022) 101228, https://doi.org/10.1016/j.uclim.2022.101228.
[9] C. Yoo, E. Cho, W. Na, M. Kang, M. Lee, Change of rainfall–runoff processes in urban areas due to high-rise buildings, J. Hydrol. 597 (2021) 126155, https://doi.org/10.1016/j.jhydrol.2021.126155.
[10] A. Beljadid, A. Hanini, An efficient semi-implicit friction source term treatment for modeling overland flow, Adv. Water Resour. 173 (2023) 104391, https://doi.org/10.1016/j.advwatres.2023.104391.
[11] J. Jeong, R.J. Charbeneau, Diffusion wave model for simulating storm-water runoff on highway pavement surfaces at superelevation transition, J. Hydraul. Eng. 136 (10) (2010) 770–778, https://doi.org/10.1061/(ASCE)HY.1943-7900.0000253.
[12] A. Kirker, L. Toran, When impervious cover doesn’t predict urban runoff: lessons from distributed overland flow modeling, J. Hydrol. 621 (2023) 129539, https://doi.org/10.1016/j.jhydrol.2023.129539.
[13] V.P. Singh, A laboratory investigation of surface runoff, J. Hydrol. 25 (3–4) (1975) 187–200, https://doi.org/10.1016/0022-1694(75)90020-7.
[14] A. Ben-Zvi, Laboratory examination of linearity in rainfall–runoff relationships, Hydrol. Sci. J. 65 (10) (2020) 1794–1801, https://doi.org/10.1080/02626667.2020.1770765.
[15] E. Straffelini, A. Pijl, S. Otto, E. Marchesini, A. Pitacco, P. Tarolli, A high-resolution physical modelling approach to assess runoff and soil erosion in vineyards under different soil managements, Soil Tillage Res. 222 (2022) 105418, https://doi.org/10.1016/j.still.2022.105418.

[16] A. Chakravarti, M.K. Jain, Experimental invesitigation and modeling of rainfall runoff process, Indian J. Sci. Technol. 7 (12) (2014) 2096–2106, https://doi.org/10.17485/ijst%2F2014%2Fv7i12%2F59445.
[17] R.J. Charbeneau, J. Jeong, M.E. Barrett, Physical modeling of sheet flow on rough impervious surfaces, J. Hydraul. Eng. 135 (6) (2009) 487–494, https://doi.org/10.1061/(ASCE)HY.1943-7900.0000043.
[18] W. Liu, W. Chen, Q. Feng, Field simulation of urban surfaces runoff and estimation of runoff with experimental curve numbers, Urban Water J. 15 (5) (2018) 418–426, https://doi.org/10.1080/1573062X.2018.1508597.
[19] W. Liu, Q. Feng, R.C. Deo, L. Yao, W. Wei, Experimental study on the rainfall-runoff responses of typical urban surfaces and two green infrastructures using scale-based models, Environ. Manage. 66 (4) (2020) 683–693, https://doi.org/10.1007/s00267-020-01339-9.
[20] V. Zhuk, L. Vovk, I. Matlai, I. Popadiuk, I. Mysak, V. Fasuliak, Dependency between the total and effective imperviousness for residential quarters of the Lviv city, J. Ecol. Eng. 21 (5) (2020) 56–62, https://doi.org/10.12911/22998993/122191.
[21] V. Zhuk, L. Vovk, I. Matlai, I. Popadiuk, Maximum daily stormwater runoff flow rates at the inlet of the Lviv WWTP based on the results of systematic hydrologic observations of the catchment, Lect. Notes Civ. Eng. 100 (2021) 514–521, https://doi.org/10.1007/978-3-030-57340-9_63.
[22] D. Li, J. Hou, Q. Zhou, J. Lyu, Zh Pan, T. Wang, X. Sun, G. Yu, J. Tang, Urban rainfall-runoff flooding response for development activities in new urbanized areas based on a novel distributed coupled model, Urban Clim. 51 (2023) 101628, https://doi.org/10.1016/j.uclim.2023.101628.
[23] K. Mazurkiewicz, M. Skotnicki, Z. Dymaczewski, Effective impervious area mapping in modeling runoff from urban catchment, Rocznik Ochrona Środowiska 22 (2020) 417–430.
[24] B. Szeląg, R. Suligowski, F. De Paola, P. Siwicki, D. Majerek, G. Łagód, Influence of urban catchment characteristics and rainfall origins on the phenomenon of stormwater flooding: case study, Environ. Model. Software 150 (2022) 105335, https://doi.org/10.1016/j.envsoft.2022.105335.
[25] P. Luo, M. Luo, F. Li, X. Qi, A. Huo, Z. Wang, D. Nover, Urban flood numerical simulation: research, methods and future perspectives, Environ. Model. Software (2022) 105478, https://doi.org/10.1016/j.envsoft.2022.105478.
[26] M. Saadi, L. Oudin, P. Ribstein, Physically consistent conceptual rainfall–runoff model for urbanized catchments, J. Hydrol. 5994 (2021), https://doi.org/10.1016/j.jhydrol.2021.126394.
[27] J.C. Guo, Storm-water predictions by dimensionless unit hydrograph, J. Irrigat. Drain. Eng. 132 (4) (2006) 410–417, https://doi.org/10.1061/(ASCE)0733-9437(2006)132:4(410).
[28] T.S. Wong, Evolution of kinematic wave time of concentration formulas for overland flow, J. Hydrol. Eng. 14 (7) (2009) 739–744, https://doi.org/10.1061/(ASCE)HE.1943-5584.0000043.
[29] Y. Xiong, C.S. Melching, Comparison of kinematic-wave and nonlinear reservoir routing of urban watershed runoff, J. Hydrol. Eng. 10 (1) (2005) 39–49, https://doi.org/10.1061/(ASCE)1084-0699(2005)10:1(39).
[30] M. Niazi, C. Nietch, M. Maghrebi, N. Jackson, B.R. Bennett, M. Tryby, A. Massoudieh, Storm water management model: performance review and gap analysis, J. Sustain. Water Built Environ. 3 (2) (2017), https://doi.org/10.1061/JSWBAY.0000817.
[31] P. Stanowska, J. Dziopak, D. Słyś, M. Starzec, An innovative rainwater system as an effective alternative for cubature retention facilities, Studia Geotechnica Mech. 43 (2021) 532–547, https://doi.org/10.2478/sgem-2021-0037.
[32] A. Deletic, The first flush load of urban surface runoff, Water Res. 32 (8) (1998) 2462–2470. https://doi:10.1016/S0043-1354(97)00470-3.
[33] L.H. Kim, M. Kayhanian, K.D. Zoh, M.K. Stenstrom, Modeling of highway stormwater runoff, Sci. Total Environ. 348 (1–3) (2005) 1–18, https://doi.org/10.1016/j.scitotenv.2004.12.063.
[34] X. Li, X. Fang, J. Li, M. Kc, Y. Gong, G. Chen, Estimating time of concentration for overland flow on pervious surfaces by particle tracking method, Water 10 (4) (2018) 379, https://doi.org/10.3390/w10040379.
[35] V. Nourani, P. Monadjemi, V.P. Singh, Liquid analog model for laboratory simulation of rainfall–runoff process, J. Hydrol. Eng. 12 (3) (2007) 246–255. https://doi:10.1061/(asce)1084-0699(2007)12:3(246).
[36] H. Aksoy, E. Unal, S. Cokgor, A. Gedikli, J. Yoon, K. Koca, B. Inci, E. Eris, A rainfall simulator for laboratory-scale assessment of rainfall-runoff-sediment transport processes over a two-dimensional flume, Catena 98 (2012) 63–72, https://doi.org/10.1016/j.catena.2012.06.009.
[37] V. Heller, Scale effects in physical hydraulic engineering models, J. Hydraul. Res. 49 (3) (2011) 293–306, https://doi.org/10.1080/00221686.2011.578914.
[38] O. Voznyak, V. Korbut, B. Davydenko, I. Sukholova, Air distribution efficiency in a room by a two-flow device, Adv. Resour. Sav. Technol. Mater. Civ. Environ. Eng. 47 (2019) 526–533, https://doi.org/10.1007/978-3-030-27011-7_67.
[39] M.L. Yakubu, Z. Yusop, Adaptability of rainfall simulators as a research tool on urban sealed surfaces–a review, Hydrol. Sci. J. 62 (6) (2017) 996–1012, https://doi.org/10.1080/02626667.2016.1267355.
[40] J.L.M.P. De Lima, V.P. Singh, Laboratory experiments on the influence of storm movement on overland flow, Phys. Chem. Earth, Parts A/B/C 28 (6–7) (2003) 277–282, https://doi.org/10.1016/S1474-7065(03)00038-X.
[41] V. Zhuk, I. Matlai, L. Vovk, I. Popadiuk, Analytical and experimental assessment of regulating volume of the stormwater storage tanks for rains of constant intensity, Lect. Notes Civ. Eng. 290 (2023) 459–469, https://doi.org/10.1007/978-3-031-14141-6_47.
[42] V.T. Chow, D.R. Maidment, L.W. Mays, Applied Hydrology, McGraw-Hill Inc, 1988, p. 572.
[43] National Engineering Handbook, Section 4: Hydrology, Soil Conservation Service, SCS USDA, Washington DC, 1985.
[44] P. Monajemi, S. Khaleghi, S. Maleki, Derivation of instantaneous unit hydrographs using linear reservoir models, Nord. Hydrol 52 (2) (2021) 339–355, https://doi.org/10.2166/nh.2021.171.
[45] J. Ramírez, Prediction and modeling of flood hydrology and hydraulics, in: E. Wohl (Ed.), Inland Flood Hazards: Human, Riparian, and Aquatic Communities, 2000, pp. 293–333. https://doi:10.1017/CBO9780511529412.012.